Second Law Analysis of a Carbon Dioxide Transcritical Power System in Low-grade Heat Source Recovery

Y. Chen *, Almaz Bitew Workie , Per Lundqvist

Div. of Applied Thermodynamics and Refrigeration, Department of Energy Technology, Royal Institute of Technology, SE-100 44 Stockholm, Sweden

Abstract

Employing Carbon dioxide as a working media in power cycles for low-grade heat source utilization has attracted more and more attentions. However, compared to other well-known cycles that employed in low-grade heat source utilizations, the information about CO_2 power cycle is still very limited. In the current work, the performance of a CO_2 power cycle in utilizing the low-grade heat sources is simulated and the results are analyzed with a focus on second law thermodynamics (i.e. exergy and entropy). Different system parameters that influencing the system exergy and entropy change are discussed.

Engineering Equation Solver (EES) is used for simulation. The simulation results show that the matching of the temperature profiles in the system heat exchangers has crucial influences on their exergy destructions and entropy generations. It is also an essential factor that influences the system thermodynamic efficiencies.

Keywords: Carbon dioxide, exergy analysis, transcritical cycle, high pressure pump

Nomenclature

EES	Engineer Equation Solver	
C	Contribution of entropy generation	%
Cp	Specific heat	kJ/kg K
GWP	Global Warming Potential	
$\dot{m}$	Mass flow rate	kg s^{-1}
ODP	Ozone Depleting Potential	
ORC	Organic Rankine Cycle	
Q	Energy	kW
SC CO_2	Supercritical carbon dioxide	
W_{exp}	Work from the expansion process	kW
W_{net}	Net work from the SC CO_2 cycle	kW
W_p	Work supply to the Pump	kW

Greek alphabet symbols

η_{exg}	Exergy efficiency	
η_{th}	Thermal efficiency	
φ	Specific exergy	kJ/kg
Φ	Exergy	kW
δ_s	Entropy generation	kJ/kg K

* Corresponding author. Tel.: +46-(0)8-790-7435 Fax: +46-8-203-007
E-mail address: yang.chen@energy.kth.se (Y. Chen)

Subscripts

a	average
a − g	Cycle working route points
c	Condenser
exp	Expander
h-h’	Cooling media condition point
gas	Heat source
gh	Gas heater
gc	Gas cooling
in	Heat exchanger inlet
is	Isentropic
out	Heat exchanger outlet
m	Mechanical
p	Pump
T	Turbine
th	Thermal
w	Water

Introduction

Energy security, economic development and environment protection are not well balanced today and the energy demand is still closely connected to the economic growth. Among the energy resources worldwide, fossil fuels still play the dominant role, which account for 77% of the increasing energy demand 2007-2030 [1] . Consequently, the dramatic increase of the energy demand due to the worldwide economic growth has caused more and more severe environmental problems, as air pollution, climate changes etc. The predicted energy related CO_2 emission will rise 130% by year 2050 and can result in a global temperature increase by 6 °C [2] .

Improving the energy efficiency by utilizing the energy in low-grade heat source / surplus heat offers a great opportunity for a sustainable energy future and less environmental problems. Figure 1 shows the typical temperature range of different renewable/ surplus heat sources. The heat sources with available temperature lower than 300 °C are normally considered as low-grade heat sources, for which conventional steam Rankin cycle is not proper for heat recovery, due to its low thermal efficiency, large volume flow and erosion of the turbine blades [3] .

Figure 1 typical temperature range of different heat sources for heat recovery[1]

[1] Pictures are from internet and only for symbolizing different heat sources

The research on low-grade heat source utilization with power cycles that utilizing CO_2 as a working fluid has caused more and more attentions in recent years. This is not only due to the reason that CO_2 is environmental benign, low-cost, non-toxic and non-flammable, but also because the supercritical CO_2 temperature profile can provide a better match to the low-grade heat source temperature profile than other working fluids that used in conventional cycles. This will help CO_2 system to reduce the irreversibility in its heating process, which gives a better thermal efficiency than the systems with conventional working fluids.

Among the research on CO_2 power cycles in low-grade heat source utilization, Zhang and his colleagues investigated the potential of CO_2 power cycle in utilizing the solar energy both theoretically and experimentally [4] -[8] . Chen et al. investigated the performance of a carbon dioxide power cycle in utilizing the low-grade heat sources and compared its performance with Organic Rankine Cycles (ORC) [9] - [11] . Moreover, Cayer and his colleagues studied CO_2 power system under fixed system working conditions and discussed system optimizations [12] . Wang et al. tried to optimize the working parameters of supercritical CO_2 power cycle under a fixed heat source condition by using genetic algorithm and artificial neural network with an assumption that the system heat exchangers will provide sufficient heating /cooling to the desired cycle working conditions [13] .

In the current study, the performance of a carbon dioxide transcritical power system is simulated with a given heat source condition. The system's performance is analyzed from a second law thermodynamic viewpoint (exergy and entropy) with a focus on the matching of the temperature profiles in the system heat exchangers and its influence on the system performance. Engineering Equation Solver (EES) is employed for the simulation.

System description

A basic CO_2 transcritical power system consists of four main components, namely a pump, a gas heater, an expansion device and a condenser. The system schematic layout and the corresponding T-S chart are shown in *Figure 2*.

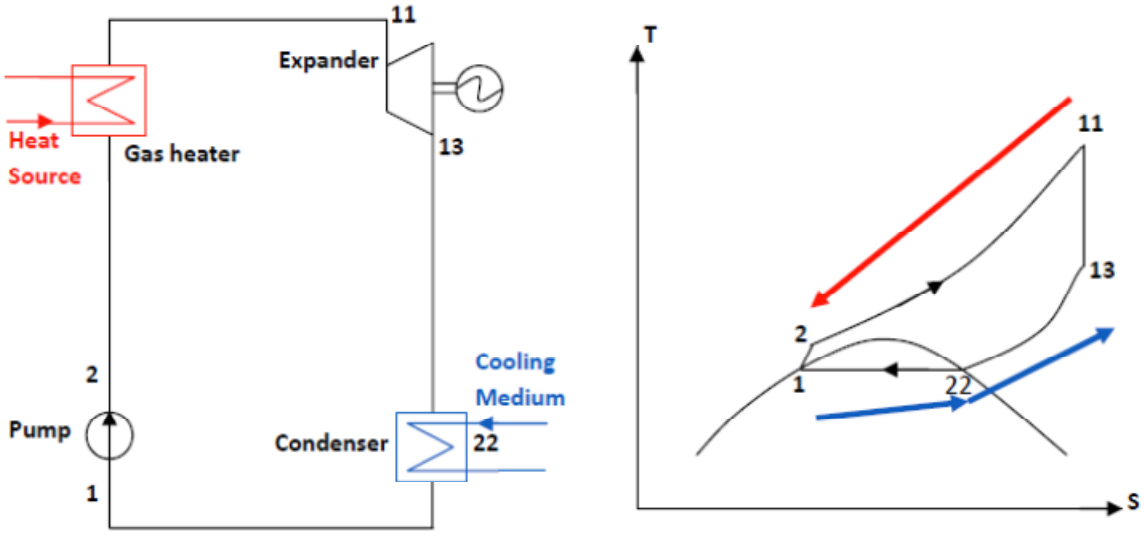

Figure 2 Schematic layout and the corresponding T-S chart of a CO_2 transcritical power system

As illustrated in the schematic *T-S* chart (Figure 2) that CO_2 still holds a high temperature at the expansion outlet (point 13), and its energy can be further recovered to produce warm water for space heating (e.g. floor heating). To be able to recover this energy sufficiently and to avoid the pinching[2]

[2] Pinching is the minimum temperature difference inside a heat exchanger , which limited the heat exchanger performance

(due to the phase changing of CO_2) in its condensing process, the condenser can be divided into two heat exchangers, namely condenser and gas cooler. Condenser will be used to condense the CO_2 from its saturated phase to the liquid phase, before it enters the pump (point 22 to point 1). The gas cooler will be used to recover the energy from expansion outlet CO_2 to produce warm water (point 13 to point 22) for space heating.

Simulation conditions description

The following general assumptions are made for the thermodynamic analysis of the cycle:

- The heat source is assumed to have an available temperature of 160 ^{o}C and a mass flow rate of 10kg/s
- The cycle is considered to work at steady state
- Pressure drops in the heat exchangers are neglected
- Isentropic efficiencies of the pump and the expansion machine are assumed to be 0.85 and 0.8 respectively and the mechanical efficiency is assumed to be 0.95 for both
- The pinching in the condenser is assumed to be 5 ^{o}C
- The condensing pressure is assumed to be 60 bar
- The cooling water inlet temperature is assumed to be 15 ^{o}C
- The set value for the water outlet temperature from the gas cooler is 50 ^{o}C

Following equations are used in the simulation model.

The heat balance of the gas heater (process 2 to 11) can be expressed as:

$$Q_{gas=}\dot{m}_{gas}Cp\left(t_{gas\ in}-t_{gas\ out}\right) \quad \text{Equation 1}$$

$$Q_{gas}=\dot{m}_{CO2}(h_{11}-h_{2}) \quad \text{Equation 2}$$

The power consumption of the pump is calculated by the following equation:

$$W_{p}=\dot{m}_{CO2}(h_{2}-h_{1})/\eta_{p,m}=\dot{m}_{CO2}\left[\left(\frac{h_{2,is}-h_{1}}{\eta_{p,is}}\right)+h_{1}\right]/\eta_{p,m} \quad \text{Equation 3}$$

The power generated by the expansion machine can be expressed as equation 4

$$W_{exp}=\dot{m}_{co2}\left[h_{11-}(h_{11}-h_{13})\eta_{t,is}\right]\eta_{m} \quad \textit{Equation 4}$$

For the condenser and gas cooler, the energy balance can be calculated by the following equations:

$$Q_{c}=\dot{m}_{CO2}(h_{22}-h_{1}) \quad \text{Equation 5}$$

$$Q_{gc}=\dot{m}_{CO2}(h_{13}-h_{22}) \quad \text{Equation 6}$$

$$Q_c = \dot{m}_{w,c} Cp_{w,c}(t_{wco} - t_{wci})$$ Equation 7

$$Q_{gc} = \dot{m}_{w,gc} Cp_{w,gc}(t_{wgo} - t_{wco})$$ Equation 8

The thermal efficiency of the power cycle can be defined by question 9

$$\eta_{th} = \frac{W_T}{Q_{gas}}$$ Equation 9

Second law thermodynamic analysis has become more and more popular in energy system analysis, since it gives a clearer picture of the system performance and its losses. Exergy concept as one of the main interests in second law system analysis can help to locate the system non-idealities by showing the significance of system components in system exergy destruction. The exergy destruction of each system component can be calculated by equation 13 generally.

$$\Delta\emptyset = \varphi_{supplied} - \varphi_{recovered}$$ Equation 10

Where

$$\varphi = (h - h_0) - T_0(s - s_0)$$ Equation 11

In the equation above, h_0 and s_0 are the enthalpy and entropy at the reference temperature (environmental temperature). Based on equation 13 and equation 14, the exergy destruction in different CO_2 power system components can be calculated (equation 15- equation 18).

$$\Delta\emptyset_{gh} = \dot{m}_{gas}(\varphi_{gasin} - \varphi_{gasout}) - \dot{m}_{co_2}(\varphi_{11} - \varphi_2)$$ *Equation 12*

$$\Delta\emptyset_{gc} = \dot{m}_{co_2}(\varphi_{13} - \varphi_{22}) - \dot{m}_{wgc}(\varphi_{wgco} - \varphi_{wco}) + \dot{m}_{co_2}(\varphi_{22} - \varphi_1) - \dot{m}_{wc}(\varphi_{wco} - \varphi_{wci})$$ *Equation 13*

$$\Delta\emptyset_p = \dot{m}_{co_2}(h_2 - h_1 - (\varphi_2 - \varphi_1))$$ *Equation 14*

$$\Delta\emptyset_{exp} = \dot{m}_{co_2}(\varphi_{11} - \varphi_{13} - (h_{11} - h_{13}))$$ *Equation 15*

The exergy efficiency of the cycle can be then defined as equation 19

$$\eta_{exg} = 1 - \frac{\sum \Delta\emptyset}{\dot{m}_{gas} \cdot \varphi_{in}}$$ Equation 16

As an alternative calculation of exergy in second law thermodynamic analysis, the entropy generation for each component can also depict a clear picture of the distribution of the irreversibility generated by each component that influence the system performance.

The entropy generation by each system component can be expressed by the following equations

$$\delta_{s,gh} = \frac{Q_{gas}}{T_{evh}} - \frac{Q_{gas}}{T_{a,g}}$$ *Equation 17*

In which

$$T_{a,gas} = \frac{h_{gas\,in} - h_{gas\,out}}{s_{gas\,in} - s_{gas\,out}}$$ *Equation 18*

$$\delta_{s,c} = \frac{Q_{gc}}{T_{a,w,gc}} - \frac{Q_{gc}}{T_{a,gc}} + \frac{Q_c}{T_{a,w,c}} - \frac{Q_c}{T_{a,c}}$$ *Equation 19*

In which

$$T_{a,w,gc} = \frac{T_{w,o}+T_{w,s}}{2} + 273 \qquad \textit{Equation 20}$$

$$T_{a,w,c} = \frac{T_{w,i}+T_{w,s}}{2} + 273 \qquad \textit{Equation 21}$$

$$T_{a,gc} = \frac{h_{13}-h_{22}}{s_{13}-s_{22}} \qquad \textit{Equation 22}$$

$$T_{a,c} = \frac{h_{22}-h_{1}}{s_{22}-s_{1}} \qquad \textit{Equation 23}$$

$$\delta_{s,p} = s_2 - s_1 \qquad \textit{Equation 24}$$

$$\delta_{s,exp} = s_{13} - s_{11} \qquad \textit{Equation 25}$$

$$\delta_{s,total} = \delta_{s,gh} + \delta_{s,c} + \delta_{s,p} + \delta_{s,exp} \qquad \textit{Equation 26}$$

Based on the equations above, the contribution from each component to the total system entropy generation can be expressed as below

$$C_{gh} = \frac{\delta_{s,gh}}{\delta_{s,total}} \qquad \textit{Equation 27}$$

$$C_{c} = \frac{\delta_{s,c}}{\delta_{s,total}} \qquad \textit{Equation 28}$$

$$C_{p} = \frac{\delta_{s,p}}{\delta_{s,total}} \qquad \textit{Equation 29}$$

$$C_{exp} = \frac{\delta_{s,exp}}{\delta_{s,total}} \qquad \textit{Equation 30}$$

By keeping the heat source inlet condition constant as 160 °C and 10 kg/s and maintaining the system pressures at 60 bar and 120 bar for heat rejecting and heat receiving processes respectively, the exergy destructions in different system components are plotted against different CO_2 mass flow rates in Figure 3.

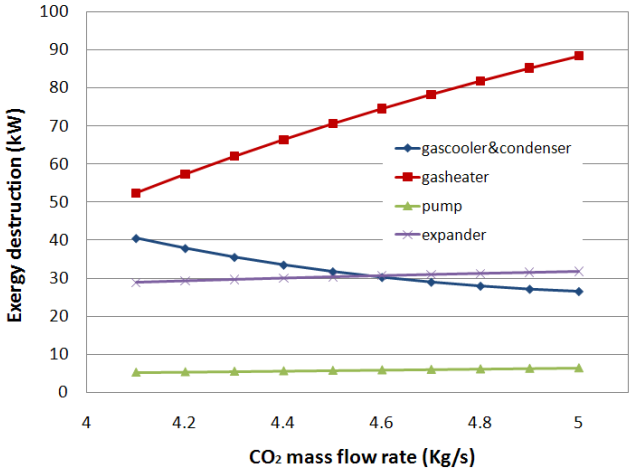

Figure 3 Exergy destruction against CO_2 mass flow rate

As shown in Figure 3 that the system's heat exchangers contribute most to the system exergy destructions. With an increasing CO_2 mass flow, the exergy destructions in the pump and the expander remain almost constant. At the same time, the exergy destruction is decreasing in the gas cooler & condenser, while increasing in the gas heater. Same trend can be found in entropy generation calculation as well (Figure 4).

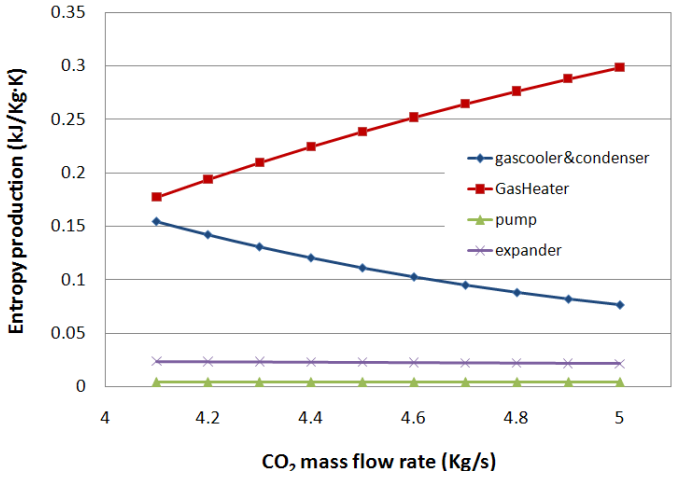

Figure 4 Entropy generation against CO_2 mass flow rate

As shown in Figure 4 that the entropy generations in the pump and the expander are almost constant with an increasing CO_2 mass flow rate. Meanwhile, as the CO_2 mass flow rate increases, the entropy generation is decreasing in the system heat rejecting heat exchangers (gas cooler & condenser), while increasing in the system heat receiving heat exchanger (gas heater).

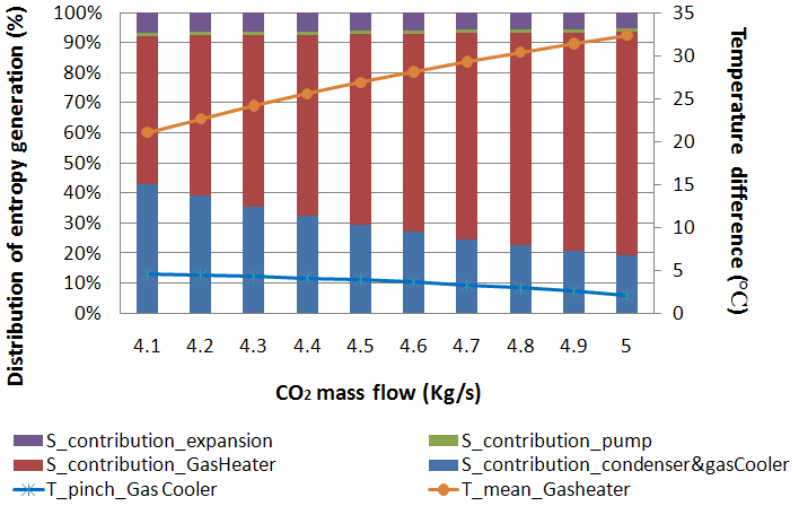

Figure 5 Distribution of entropy generation vs. CO_2 mass flow

Figure 5 shows the distribution of entropy generation by different system components as well as the pinching in the gas cooler and the mean temperature difference in the gas heater against different CO_2 mass flow rates. As indicated in the figure that the contributions of the entropy generations from the pump and the expander are relative small and almost constant. While the contributions of the entropy generations from the gas cooler & condenser and the gas heater are dominating.

Comparing Figure 3, Figure 4 and Figure 5, one may notice that the exergy destruction and the entropy generation in the heat exchangers are closely related to the matching of the temperature files in them (i.e. pinching and mean temperature difference). With an increasing CO_2 mass flow, the mean temperature difference in the gas heater is increasing (i.e. the temperature profiles of the heat source and SC CO_2 are departing from each other). Nevertheless, pinching in the gas cooler is decreasing (i.e.

the temperature profiles of the water and CO_2 are getting closer). As a consequence, the exergy destruction and the entropy generation are increasing in the gas heater, while decreasing in the gas cooler & condenser with the increasing CO_2 mass flow rate. This also leads to an increasing contribution of entropy production from the gas heater, but a decreasing contribution from the gas cooler & condenser (Figure 5).

Furthermore, by plotting the system thermal efficiency and the exergy efficiency against different CO_2 mass flow rates, it can be found that the system thermodynamic efficiencies are slightly decreasing with increasing CO_2 mass flow rate.

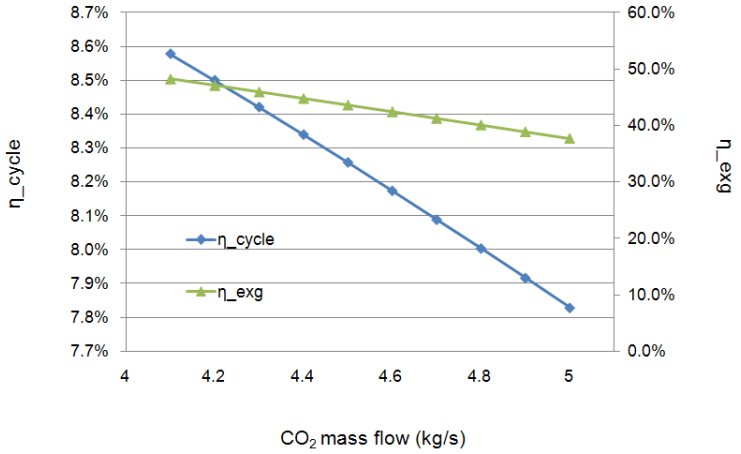

Figure 6 System thermodynamic efficiencies vs. CO_2 mass flow

By maintaining cycle simulation conditions as stated in the assumptions, while changing the system high pressure side pressure, the exergy destruction in different system components are plotted in Figure 7.

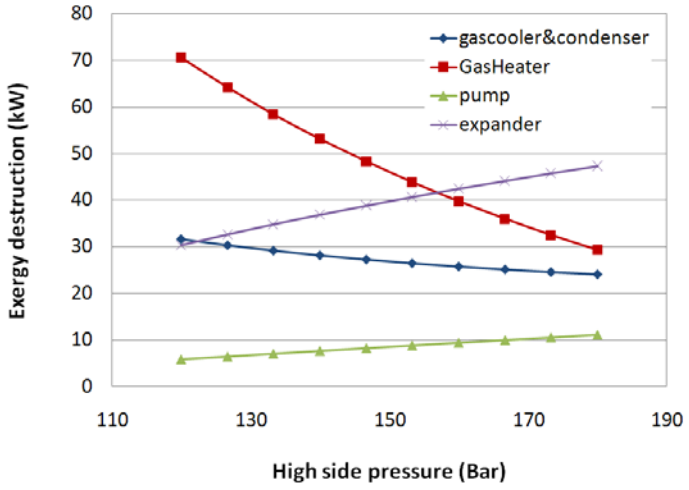

Figure 7 Exergy destruction against system high pressure side pressure

As shown in the figure that with increasing system high pressure side pressure, the exergy destructions in the expander and the pump are both increasing, while the exergy destructions are decreasing.

Same trend can also be seen in the simulation results of entropy generations from different system components against different system high pressure side pressures (Figure 8). As shown in Figure 8 that the entropy generations in the expander and the pump are both increasing, while the entropy generations in the system heat exchangers are decreasing.

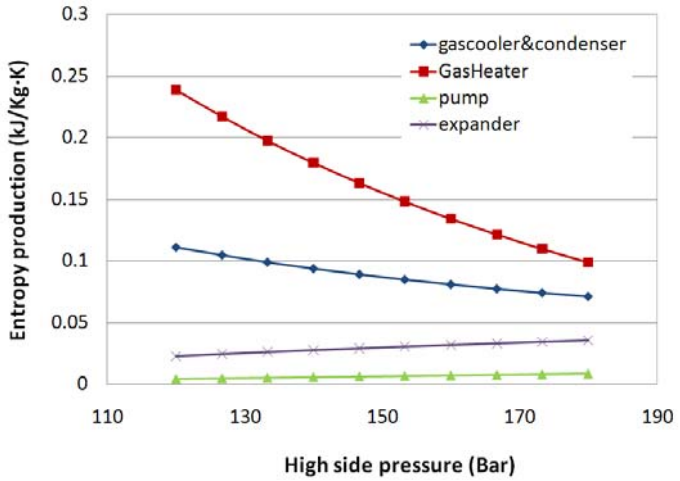

Figure 8 Entropy generation vs. system high pressure side pressure

Figure 5 shows the distribution of entropy generation by different system components as well as the pinching in the gas cooler and the mean temperature difference in the gas heater against different system high pressure side pressures.

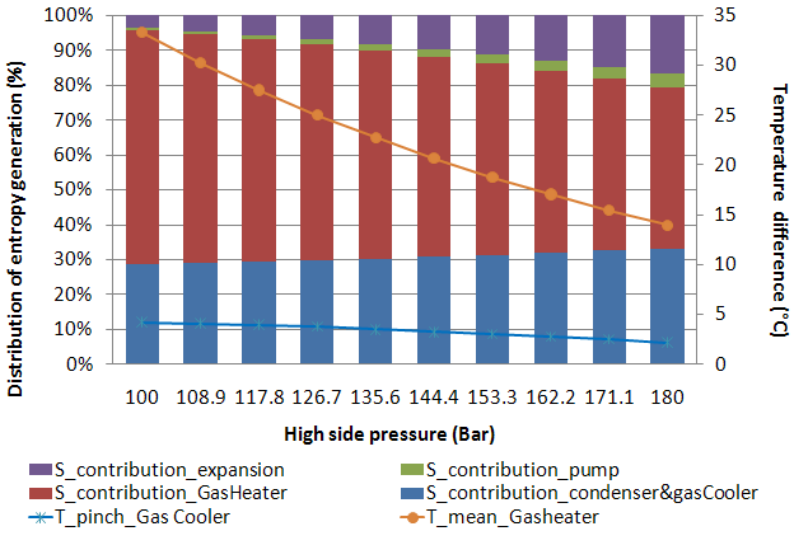

Figure 9 Distribution of entropy generation vs. system high pressure side pressure

Combining Figure 7, Figure 8 and Figure 9, it can be found again that the changes of exergy destruction and entropy generation in the system heat exchangers are closely related to the matching of the temperature profiles in them. With a decreasing pinching in the gas cooler and a decreasing mean temperature difference in the gas heater, the exergy destruction and entropy production are both decreasing in the system heat exchangers.

Due to the decrement of entropy generation is more obvious in the gas heater than in the gas cooler & condenser with the increasing system high pressure side pressure, the distribution of the entropy generation for the gas cooler & condenser is increasing, while by the gas heater is decreasing. Meanwhile the distribution of entropy generations by the pump and the expander are increasing and the increment is more obvious for the expander (Figure 10).

By plotting the cycle thermal efficiency and exergy efficiency against different system high pressure side pressures, it is found that the system thermodynamic efficiencies are increasing with increasing system high pressure side pressure.

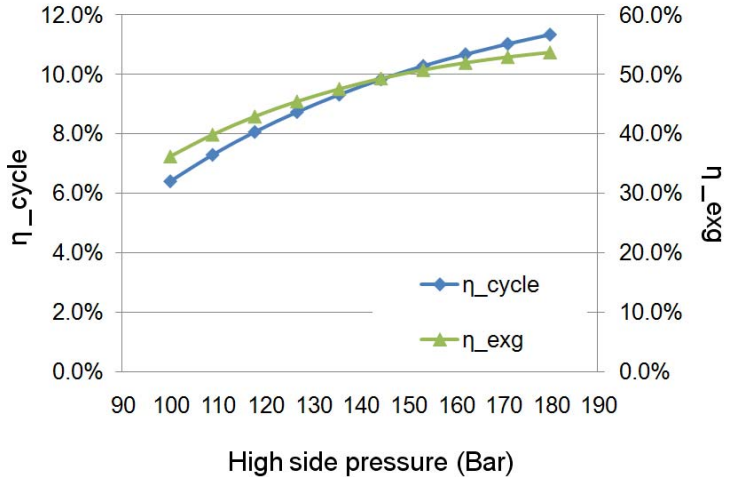

Figure 11 System thermodynamic efficiencies vs. system high pressure side pressure

By keeping the heat source mass flow constant at 10kg/s and maintaining the system pressures at 60 bar and 120 bar for the system heat rejecting and heat receiving heat exchangers respectively, the exergy destructions in different system components are plotted against different heat source temperatures at the gas heater inlet.

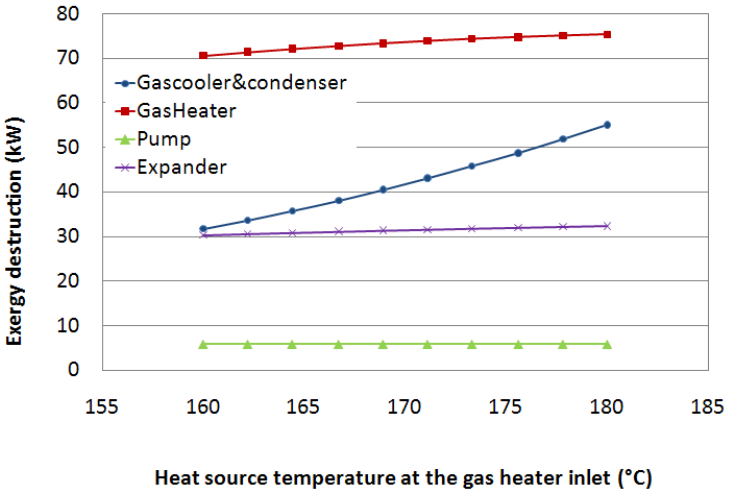

Figure 12 Exergy destruction vs. heat source temperature at the gas heater inlet

It can be seen from Figure 12 that with an increasing heat source inlet temperature, the exergy destructions in the pump and the expander are almost constant. The exergy destruction in the gas heater is slightly increasing, but the increasing trend is less obvious at higher heat source inlet temperatures. The exergy destructions in the gas cooler & condenser are increasing more obviously with the increasing heat source temperature.

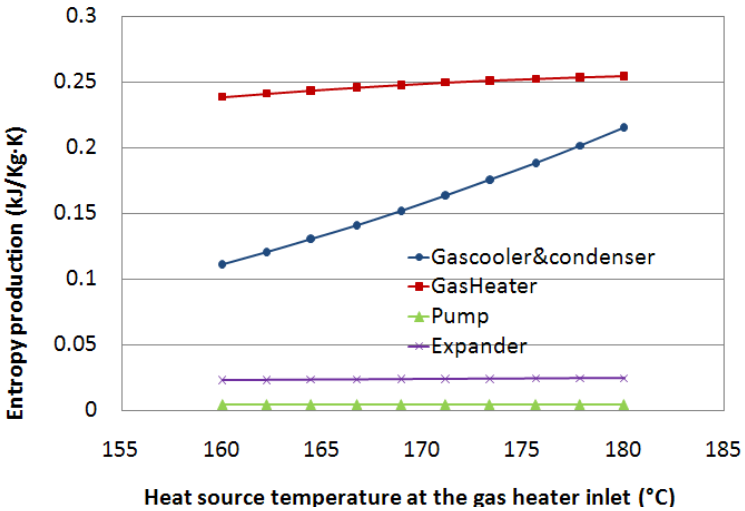

Figure 13 Entropy generation vs. heat source temperature at the gas heater inlet

Figure 13 shows the entropy production in different system components against the heat source temperature at the gas heater inlet and same trend as exergy destruction can be found. The entropy generation in the pump and the expander are almost constant, while in all the heat exchangers are increasing.

Figure 14 shows the distribution of entropy generation by different system components as well as the pinching in the gas cooler and the mean temperature difference in the gas heater against different heat source temperatures at the gas heater inlet.

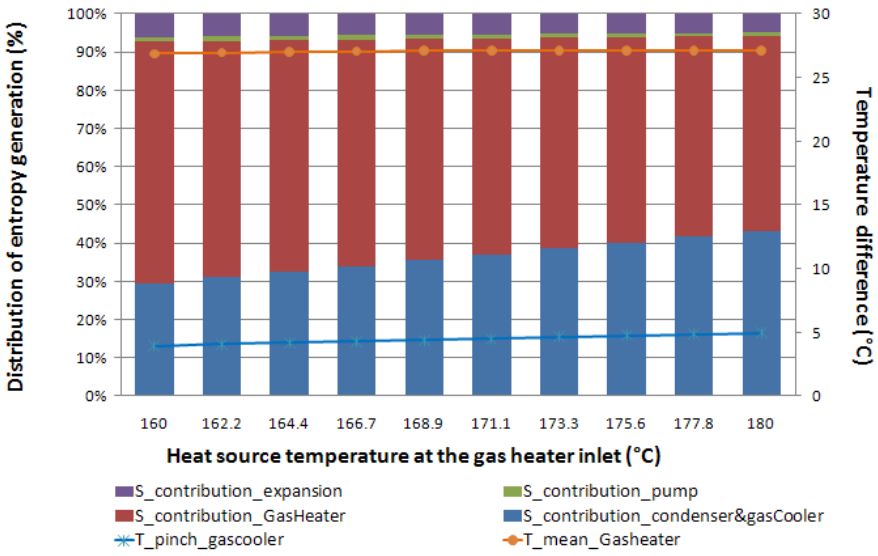

Figure 14 Entropy generation vs. heat source inlet temperature

Combining Figure 12, Figure 13 and Figure 14, the influence of the temperature profile's matching on the heat exchangers' exergy destructions and entropy generations can be noticed again. With an increasing pinching and an increasing mean temperature difference, both the exergy destruction and the entropy generation are increasing in all the system heat exchangers. However, due to the increment is more obvious in the gas cooler & condenser than in the gas heater, the distribution of the entropy generation by the gas cooler & condenser is increasing , while by the gas heater is decreasing instead. Furthermore, the distribution of the pump is constant and of the expander is slightly decreasing.

By plotting the system thermal efficiency and exergy efficiency against different heat source temperatures at the gas heater inlet, it can be found that the system thermodynamic efficiencies are increasing with the increasing heat source temperature.

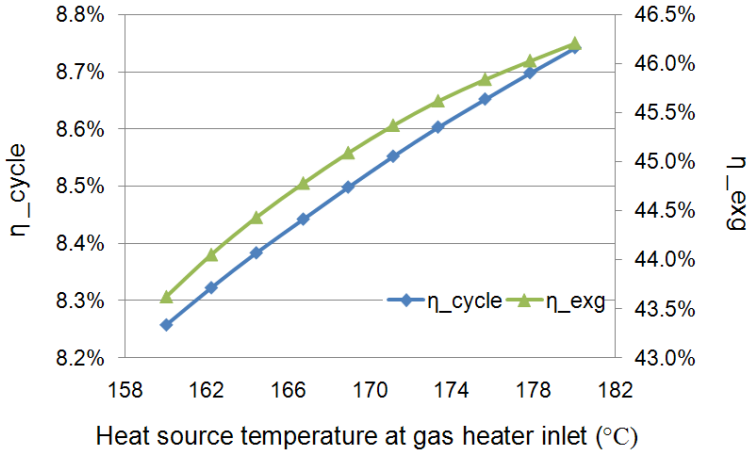

Figure 15 System thermodynamic efficiencies vs. heat source inlet temperature

Conclusions

In the current study, the performance of a supercritical CO_2 power cycle in utilizing the energy in low-grade heat sources is analyzed from the second law thermodynamic viewpoint. The influences of different system working parameters on the system exergy and entropy changes are simulated and discussed.

Remaining other system working conditions and the heat source inlet conditions constant, while changing the CO_2 mass flow rate, it can be noticed that the exergy destruction and the entropy generation in the expander and the pump are almost constant with an increasing CO_2 mass flow rate. Furthermore, the exergy destruction and the entropy generation are increasing in the system gas heater, but decreasing in the gas cooler & condenser. The contributions of entropy generations from the expander and the pump are and are almost independent on the CO_2 mass flow rate. On the contrary, the contributions of the entropy generations by the heat exchangers are high and is decreasing from the gas cooler & condenser, while increasing from the gas heater with an increasing CO_2 mass flow rate. Moreover, the system thermodynamic efficiencies (thermal efficiency and exergy efficiency) are slightly decreasing with the increasing CO_2 mass flow rate.

By plotting the system performance with different system high pressure side pressures, it can be found that the exergy destruction and the entropy generation are increasing in the expander and the pump, while decreasing in the gas heater and the gas cooler & condenser. For the distribution of the entropy generation in the system, it can be found that the distributions are increasing for the expander, the pump, and the gas cooler & condenser, while decreasing for the gas heater with the increasing system high pressure side pressure. The different trend between the gas heater and the gas cooler & condenser is due to the decrement of the min temperature difference in the system heat exchanger is more obvious in the gas heater than in the gas cooler & condenser. For the system thermodynamic efficiencies, both system thermal efficiency and the exergy efficiency are increasing with the increasing system high pressure side pressure.

Maintaining other system working parameters constant, the system performances with increasing heat source inlet temperature are simulated. It can be found that the exergy destruction and the entropy generation are increasing in all the system components, although the increasing trend is more obvious in the gas cooler & condenser than in other components. The plot of the distribution of entropy generation shows that the distribution is increasing for the gas cooler & condenser, while decreasing

for other components. It is also found that both the system thermal efficiency and the system exergy efficiency are increasing with the increasing heat source temperature.

In general, all the simulation results indicate that the matching of the temperature profiles in the system heat exchangers has crucial influence on their exergy destructions and entropy generations.

Acknowledgements

The research presented in this paper is financially supported by the CREATIVE project funding. The authors would like to thank CREATIVE for the sponsorship.

References

[1] http://www.worldenergyoutlook.org/docs/weo2009/fact_sheets_WEO_2009.pdf

[2] Scientific facts on Energy Technologies Scenarios to year 2050, http://www.greenfacts.org/en/energy-technologies/energy-technologies-greenfacts.pdf

[3] Chen Y. Novel Cycles Using Carbon Dioxide as Working Fluid: New Ways to Utilize Energy from Low-grade Heat Sources, Licentiate Thesis, The Royal Institute of Technology (KTH), 2006, Stockholm.

[4] Zhang XR, Yamaguchi H, Uneno D, Fujima K, Enomoto M, Sawada N. Analysis of a novel solar energy-powered Rankine cycle for combined power and heat generation using supercritical carbon dioxide. Renewable Energy 31(2006),1839–1854.

[5] Yamaguchi H, Zhang XR, Fujima K, Enomoto M, Sawada N. Solar energy powered Rankine cycle using supercritical CO2. Applied Thermal Engineering 26 (2006), 2345–2354.

[6] Zhang XR, Yamaguchi H, Fujima K, Enomoto M, Sawada N. Theoretical analysis of a thermodynamic cycle for power and heat production using supercritical carbon dioxide. Energy 32(2007) 591–599.

[7] Zhang XR, Yamaguchi H, Uneno D. Thermodynamic analysis of the CO_2-based Rankine cycle powered by solar energy. International Journal of Energy 31(2007) 1414–1424.

[8] Zhang XR, Yamaguchi H, experimental study on the performance of solar Rankine system using supercritical CO_2. Renewable Energy 32 (2007), 2617–2628

[9] Chen Y, Lundqvist P, Platell P., Theoretical research of carbon dioxide power cycle application in automobile industry to reduce vehicle's fuel consumption, Applied Thermal Engineering 25 (2005) 2041–2053

[10] Chen Y, Lundqvist P, Johansson A, Platell P., A comparative study of the carbon dioxide transcritical power cycle compared with an organic Rankine cycle with R123 as working fluid in waste heat recovery. Applied Thermal Engineering 26 (2006) 2142–2147

[11] Chen Y, Pridasaws W., Lundqvist P., Dynamic simulation of a solar-driven carbon dioxide transcritical power system for small scale combined heat and power production, Solar Energy 84 (2010) 1103–1110

[12] Cayer E., Galanis N., Desilets M., Nesreddine H, Roy P., Analysis of a carbon dioxide transcritical power cycle using a low temperature source, Applied Energy 86 (2009) 1055–1063

[13] Wang J.F., Sun Z.X., Dai Y.P., Ma S.L., Parametric optimization design for supercritical CO_2 power cycle using genetic algorithm and artificial neural network, Applied Energy 87 (2010) 1317–1324